MURAJ
Minnesota Undergraduate Research & Academic Journal
z.umn.edu/MURAJ

Inhibition of MCT1 to Reduce Tumor Invasion During Early Malignant Progression in HNSCC

By Ethan J. Wong[1], Ali Khammanivong[1], Erin B. Dickerson[1,2]

[1]Department of Veterinary Clinical Sciences, College of Veterinary Medicine
[2]University of Minnesota, St. Paul MN; Masonic Cancer Center, University of Minnesota, Minneapolis, MN

Abstract: Head and neck squamous cell carcinoma (HNSCC) is a widespread and common cancer, ranking as the sixth most prevalent form of cancer within the last decade. Treatment resistance and tumor persistence are large contributing factors to the mortality of HNSCC. One mechanism of treatment resistance is the maintenance of stem cell-like properties of cancer cells and their subsequent adaptability to changes in the tumor microenvironment (TME). Monocarboxylate transporter-1 (MCT1) is an important transport protein that aids in cancer cell invasion, supports cell growth, and improves cell adaptivity in the TME through transport of important monocarboxylates. This study aimed to inhibit MCT1 both genetically through CRISPR/Cas9 gene editing and pharmacologically through use of AZD3965, an MCT1 inhibitor, in order to measure the effect of cancer cell invasion and determine if MCT1 can be a therapeutic target for HNSCC. Genetic knockout of MCT1 led to substantial decreases in invasion of an HNSCC cell line; pharmacological inhibition of MCT1 also decreased invasion, though not significantly. These findings suggest that MCT1 plays a major role in the invasion of HNSCC cells and targeting this protein may provide novel solutions to treating resistant HNSCC.

Introduction

Head and neck squamous cell carcinoma (HNSCC), which includes oral and oropharyngeal carcinomas, is a highly aggressive and invasive disease. HNSCC is a major health problem worldwide due to the heterogeneity in the disease etiology and treatment responses, as well as the persistence of tumor progression. HNSCC has been found to be highly correlated to alcohol and tobacco use as well as infection with human papilloma viruses HPV-16 and HPV-18 (Stein et al., 2015). Because of the wide range of causes of HNSCC, the disease was found to be the sixth highest form of cancer worldwide in 2018 with predictions estimating a 30% increase in the prevalence

worldwide by 2030 (Johnson et al., 2020). Current treatment of HNSCC involves the use of platinum-based chemotherapies, such as cisplatin, but this can lead to chemotherapy resistance and eventual recurrence (Picon and Guddati, 2020). Treatment resistance and tumor persistence in HNSCC may reflect properties of cancer stem cells (CSCs), which are thought to be the main contributors to the underlying mechanisms of oncogenic progression, invasion, and recurrence in HNSCC (Baniebrahimi et al., 2020; Chen and Wang, 2019). One crucial stem cell-like property is the maintenance of a tumor cell de-differentiated state, where metabolic reprogramming occurs to support long-term survival, invasion, and tumor growth under varying tumor microenvironments (TME) (Cho et al., 2015). Additionally, HNSCC tumors that are associated with high levels of hypoxia are known to have worsened prognoses and increased resistance to radiotherapy (Brizel et al., 1997). The mechanism of treatment resistance occurs through induction of transcription factor subunit HIF1α, which drives angiogenesis and upregulates expression of genes contributing to metabolic reprogramming from oxidative phosphorylation to glycolysis (Alsahafi et al., 2019).

Monocarboxylate transporter 1 (MCT1; encoded by the *SLC16A1* gene) is a member of the solute carrier 16 family of proteins (Halestrap, 2013a, 2013b). Its function is to transport important carboxylate metabolites such as L-lactate, pyruvate, and β-hydroxybutyrate into and out of the cell, which aids in cell function and metabolism (Halestrap and Meredith, 2004). Previous studies have shown that MCT1 is expressed primarily in the basal layer of the mucosal tissues and is often elevated in HNSCC (Curry et al., 2013; Khammanivong et al., 2016). Several genes including *SLC16A1*, inhibin beta A (*INHBA*), laminin gamma 2 (*LAMC2*), and cell surface glycoprotein (CD44) have been shown to act as genetic markers for HNSCC and are significantly upregulated in HNSCC samples (Khammanivong et al., 2014, 2016). Expression of MCT1 is strongly and positively correlated with that of a cell surface glycoprotein CD44, a marker for CSCs in HNSCC (Khammanivong et al., 2014). Both CD44 and MCT1 expression and signaling are known to be associated with tumor initiation, proliferation, and interaction with the TME in HNSCC (Krishnamurthy and Nör, 2012; Prince et al., 2007; Sayed et al., 2011; Siegel et al., 2017). Because MCT1 is a proton-linked membrane transporter that moves carboxylate metabolites in and out of cells as energy sources as well as for extracellular restructuring to support growth and invasion (Halestrap, 2013a, 2013b; Sonveaux et al., 2008), we sought to target MCT1 and determine whether invasion of HNSCC can be blocked through both genetic and pharmacological means. By targeting MCT1, and thus CSCs, tumor persistence and progression may be prevented, allowing for development of novel therapies for HNSCC and address concerns of the growing prevalence of HNSCC.

Methods

Cell lines and culture conditions: Two cell types were used for this study: TR146, an invasive human HNSCC cell line (Provided by Dr. Mark Herzberg, University of Minnesota; Rupniak et al., 1985), and human pre-

cancerous dysplastic oral keratinocyte (DOK; Sigma-Aldrich). TR146 cells were used to model cancer cell invasion while DOK cells were used to model invasion of pre-cancerous, keratinocytes to examine the efficacy of MCT1 targeting before cancer occurs. TR146 cells were grown in Dulbecco Modified Eagle Medium (DMEM) and supplemented with 10% fetal bovine serum (FBS) (Atlas Biologicals, Fort Collins, CO, USA) and 0.1% Primocin® (Invivogen, San Diego, CA, USA) by volume. DOK cell lines were grown in Dulbecco Modified Eagle Medium (DMEM) and supplemented with 10% FBS, 0.2% Primocin®, 0.1% human insulin, and 0.025% hydrocortisone by volume. Cells were maintained in a humidified incubator at 37 ºC and 5% CO_2. All other reagents were from Sigma-Aldrich (St. Louis, MO, USA).

CRISPR/Cas9 SLC16A1 Knockout: Knockout (KO) of MCT1 gene, *SLC16A1,* was performed through the Masonic Cancer Center Genome Engineering Shared Resource (GESR), University of Minnesota. The guide RNA (5'-GCGAAGTGTCATGGATATCC-3'), designed to target exon 2 of the *SLC16A1* gene, was co-transfected with Cas9 to induce inactivating mutations through a double-stranded break and non-homologous end joining (NHEJ) repairs. NHEJ-associated mutations were confirmed by sequencing using a primer set (Forward: 5'-GCGAAGTGTCATGGATATCC-3'; reverse: 5'-TGAGGGACCTTGATTTGCTCC-3') flanking the target site. Clonal selection was performed to identify transfected cells with an inactivating mutation. Multiple clones were selected and expanded in culture to further confirm KO of *SLC16A1* and MCT1 expression by quantitative reverse-transcription polymerase chain reaction (qRT-PCR) and immunoblotting, respectively.

qRT-PCR: qRT-PCR was performed to validate the loss in expression of *SLC16A1* as well as to evaluate the response of related genes, *LAMC2* and *INHBA*. TR146 and DOK cell lines were grown using high glucose DMEM and harvested at 80% confluency. RNA extraction was performed using Qiagen RNeasy Mini Kit™ (Qiagen, Hilden, Germany). RNA concentration was measured via spectrophotometry at 260 nm. cDNA was prepared using SuperScript™ VILO™ cDNA Synthesis Kit (Themo Fisher Scientific, Waltham, MA, USA) from RNA samples using the suggested thermocycler profile. qRT-PCR was performed using FastStart Universal SYBR™ Green Master (Roche; Basel, Switzerland) using primers for the following genes: *SLC16A1*, *LAMC2*, INHBA, and GAPDH for control. Quantification of relative mRNA expression utilized comparison of quantification cycle values (ΔCq) between GAPDH control and target gene. Standard error and related statistics were calculated across two or more days with experimental conditions performed in triplicates.

Immunoblotting: Immunoblotting was performed to confirm absence of MCT1 expression on the protein level. Cells were grown to 80% confluence prior to harvest and cell pellets were frozen at -80 ºC. Protein lysates were obtained using frozen cell pellets via Transmembrane Protein Extraction Reagent (FIVEphoton Biochemicals; San Diego, CA, USA). Protein concentration was standardized using Pierce® bicinchoninic acid (BCA) Protein Assay (Thermo Fisher Scientific). A sodium

dodecyl sulphate–polyacrylamide gel electrophoresis (SDS-PAGE), denaturing protein gel was used for gel electrophoresis, specifically, Mini-PROTEIN TGX precast protein gels (4%-15%) (BioRad, Hercules, CA, USA). Odyssey® Protein Molecular Weight Marker (LI-COR Biosciences, Lincoln, NE, USA) was used to approximate protein molecular weight. 1x SDS was used as running buffer and transferred using a semi-dry technique to a nitrocellulose membrane. Membranes were blocked for 1 hour to overnight using Odyssey Blocking Buffer in equal parts Tris- buffered saline (TBS) (LI-COR). Immunoblotting was performed using SNAP id (Sigma-Aldrich) and with anti-MCT1 rabbit polyclonal primary antibody at 1:1000 (Origene, Cat No. TA321555; Rockville, MD) and anti-β-actin mouse monoclonal primary antibody at 1:1000 (Sigma-Aldrich; St. Louis, MO). Secondary antibodies included polyclonal goat anti-Rabbit IgG (at 1:5000 dilution) and IRDye® 680LT Goat (polyclonal) Anti-mouse IgG (at 1:5000 dilution) (LI-COR). Immunoblotting was detected with Odyssey infrared scanning system (LI-COR).

MCT1 Pharmacological Blockade: MCT1 was inhibited pharmacologically in both DOK, pre-malignant, and TR146, invasive HNSCC cells to measure the efficacy of pharmacologically blocking MCT1 activity in the progression of HNSCC. A small-molecule MCT1-specific inhibitor, AZD3965 (AstraZeneca, Cambridge, United Kingdom; Cat No. S7339, Lot No. 04, via Selleckchem.com, Houston, TX) was used to block MCT1 transporter activities.

Cell Viability Assay: To determine the concentration at which AZD3965 is toxic to cells, a tetrazolium-based, colorimetric, MTS assay (CellTiter 96® AQ_{ueous} Assay; Promega, Madison, WI, USA) was used to quantify viable cells after a 72-hour treatment of AZD3965. Both TR146 and DOK cells were used to quantify the toxicity levels of AZD3965. Cells were harvested and adjusted using Countess 3 automated cell counter (Thermo Fisher Scientific) to control for cell number. Cells were then treated with AZD3965 and incubated at 37 ºC and 5% CO_2 for 72 hours. MTS reagent was added at 25 µM after 72-hour incubation. Absorbance was measured at 490 nm using TECAN Infinite m200 PRO plate reader (Tecan, Morrisville, NC, USA). Cell controls contained no added AZD3965, and background controls contained no cells, only cell culture medium and MTS.

Invasion assay: MCT1-KO and AZD3965-treated DOK and TR146 cells were tested for invasion using Transwell invasion assays to measure the effect of genetic knockout and pharmacological blockade of MCT1. TR146 and DOK cells were grown in high glucose DMEM media at 80% confluency prior to cell harvest. Cells were harvested and normalized to 50,000 cells/well in serum free medium and plated on Transwell Fluoroblok (Corning; Corning, NY, USA) membranes containing 25 µL of 3 µg/µL Matrigel coating per Transwell insert. Inserts were placed in complete medium containing FBS to induce invasion. Cells were incubated at 37 ºC overnight to allow invasion to occur. For treatment with AZD3965, cells were prepared exactly as described above except that 50 µM of AZD3965 was added to the

serum free medium during plating. Inserts were stained with Calcein AM (blue or green) (Thermo Fisher Scientific) at 5 µM to visualize viable, invasive cells using fluorescence microscopy from the bottom of the insert. Quantification of invaded cells was performed using ImageJ automated cell counting in which detection thresholds were held consistent and only cells that were greater than 100 pixels in area were counted. Statistical analysis was performed via Excel using a two tailed t-test with equal variance assumed.

Results

To evaluate the role of MCT1 in the invasion of HNSCC cell lines, KO of the *SLC16A1* gene was performed via CRISPR and confirmed through qRT-PCR and immunoblotting. Two TR146 and five DOK

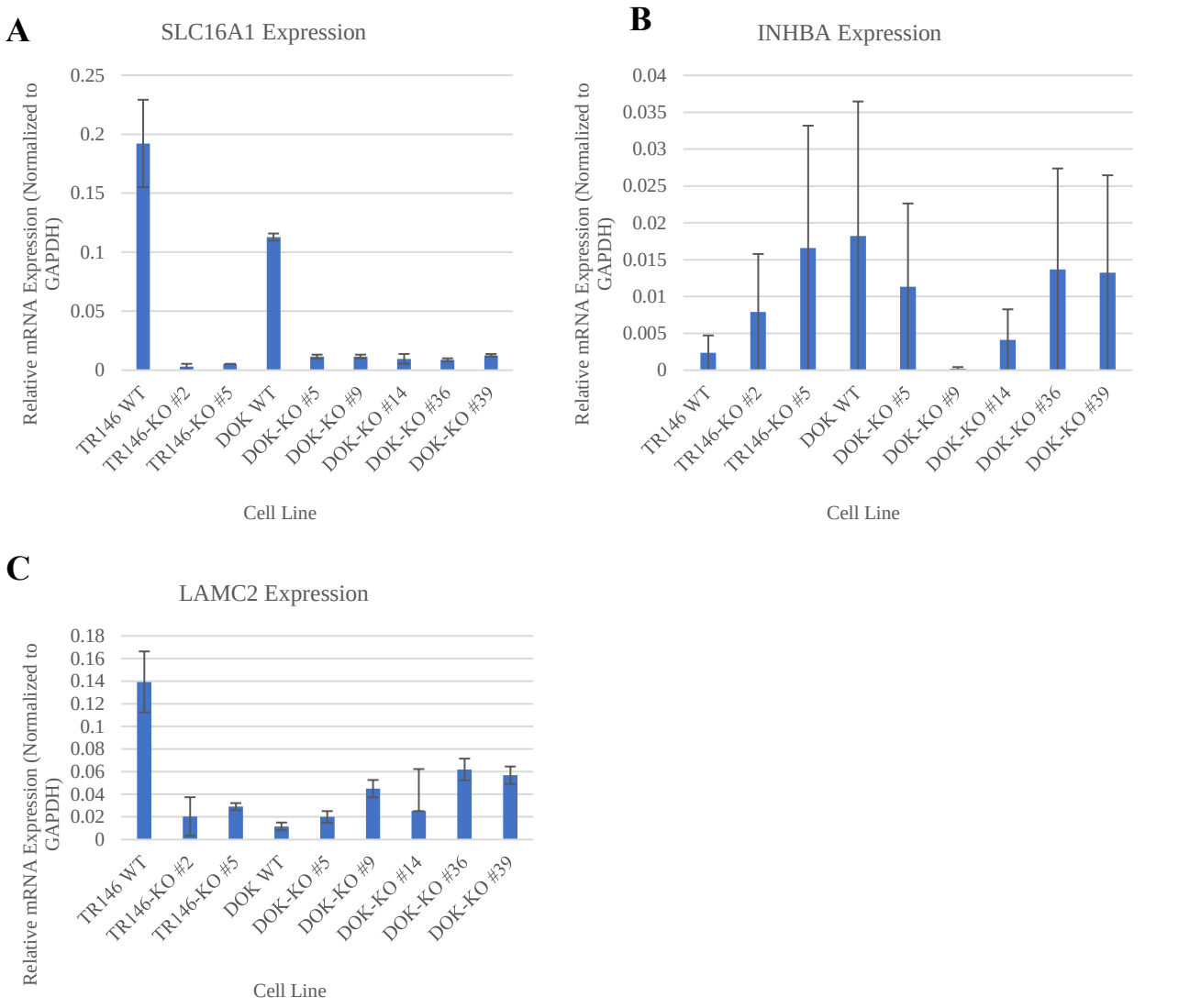

Figure 1. *qRT-PCR of TR146 and DOK cell line KOs for SLC16A1 and HNSCC marker genes*. qRT-PCR was performed to measure the relative mRNA expression for the following genes: A) *SLC16A1*, B) *LAMC2*, and C) *INHBA*. Relative expression is given by ΔCq between the target gene and GAPDH control. Standard error bars were calculated across multiple day and intra-day replicates.

MCT1 CRISPR KO clones were identified as knockouts for MCT1 and used to compare relative expression. Validation of the CRISPR KO was evaluated on the transcript level using qRT-PCR (Figure 1). Results showed a marked decrease in relative gene expression of *SLC16A1* between KO and wild type (WT) cells for both TR146 and DOK. Of the TR146 cell line, MCT1-KO clone #2 showed the greatest reduction in gene expression of *SLC16A1* as compared to the controls. For the DOK cell line, MCT1-KO clone #36 showed the lowest expression of *SLC16A1* as compared to controls. Analysis of HNSCC invasion marker gene, *LAMC2*, showed inconsistent patterns with gene expression, being largely decreased in TR146 MCT1 KOs, but upregulated in DOK MCT1 KOs. INHBA, another marker of HNSCC, also showed irregular expression with increased expression in TR146 KOs, but slight decreases in DOK MCT1 KO clone #9 and #14.

Next, SDS-PAGE and immunoblotting were used to qualitatively measure protein expression of MCT1. TR146 WT and DOK WT samples were used as positive controls for comparison of MCT1 expression. MCT1 expression was not detected in KO cells when compared to the parental, WT cells. Green bands in WT samples correlated to approximately 40-44 kDa, which matches expectations of MCT1 molecular weight given by the Origene anti-MCT1 primary antibody (37-44 kDa). Visualization via immunoblotting thus supports qRT-PCR data on the protein level, indicating marked decreases of MCT1 expression (Figure 2).

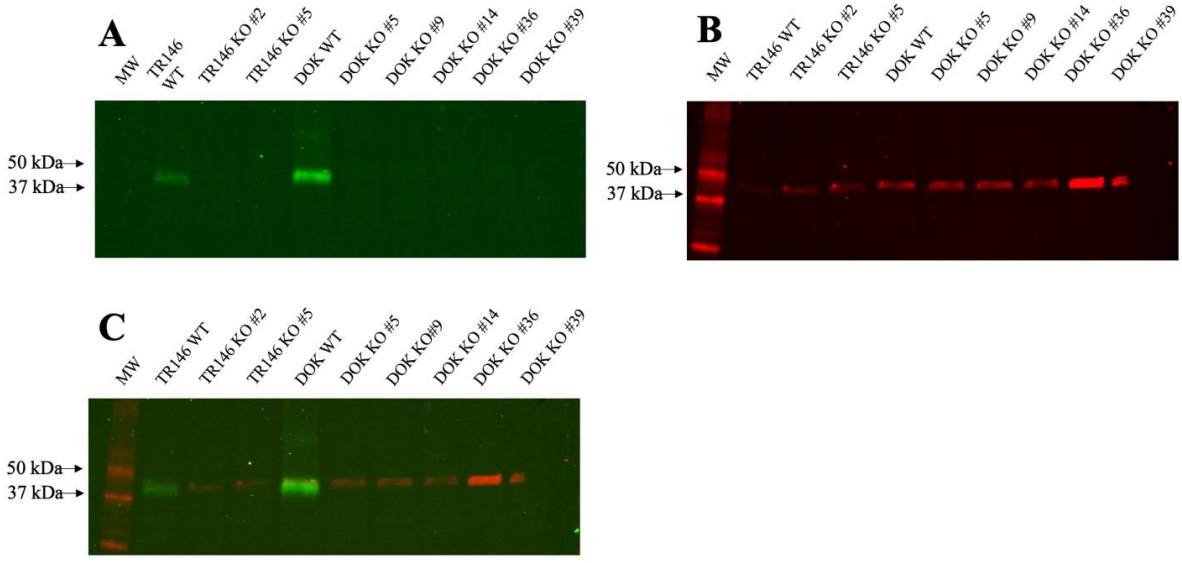

Figure 2. Immunoblotting of MCT1 in the TR146 and DOK cell lines. SDS-PAGE and immunoblotting were used to detect changes in the expression of MCT1. A) MCT1 detection at 800 nm corresponding to green bands. B) β-actin detection at 700 nm corresponding to red bands. C) Overlay of both MCT1 and β-actin expression. Molecular weight is denoted as MW.

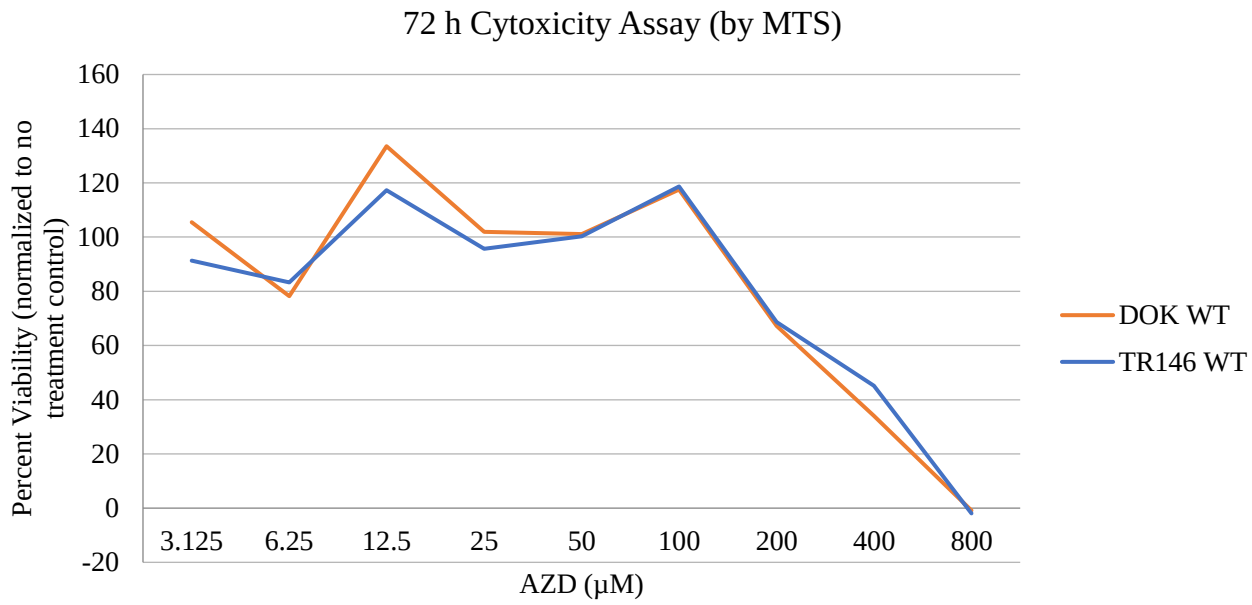

Figure 3. Cell viability Assay by MTS. Cell viability was measured after treatment with AZD3965 (µM) by MTS reagent. Viability is presented as percent viability cells normalized to control groups without treatment of AZD3965.

Treatment of AZD3965 was used to evaluate the effect of pharmacological blockade of MCT1 and measure the levels of invasion upon treatment. An MTS assay was used to establish a kill-curve of AZD3965 and determine lethal concentrations of AZD3965. Complete loss of cell viability was observed at a concentration of 800 µM AZD3965, while viability began to decrease at a concentration of 100 µM (Figure 3). IC50 values indicating the concentration of AZD3965 to achieve 50% cell viability were calculated for TR146 WT and DOK WT and found to be 410 µM and 385 µM, respectively.

To measure and compare the levels of invasion of TR146 and DOK cell lines between WT and KO cells, an invasion assay was performed to measure migration through a Matrigel matrix. Marked and significant decreases in invasion by MCT1-KO TR146 cells were observed as compared to the WT control. Invasion in TR146 WT was widespread and highly uniform across the membrane (Figure 4A). WT cells maintained consistent density in areas of migration through the Matrigel matrix. KO clones, however, showed large decreases in the density of invasive cells across the membrane. While comparable KO of MCT1 was observed in both clone #2 and #5, clone #5 was less invasive compared to clone #2 (Figure 4B-C). Invasion was not observed in the WT and KO DOK cell lines.

To confirm these results, pharmacological blockade of MCT1 was performed using AZD3965 in combination with the invasion assay (Figure 5). Drug treatment decreased the invasion and migration of TR146 and DOK cells in some instances while differences were not observed in others. On some single day replicates, extensive decreases in invasion between control and AZD3965 treated cells were noted (Figure 5). Other replicates with

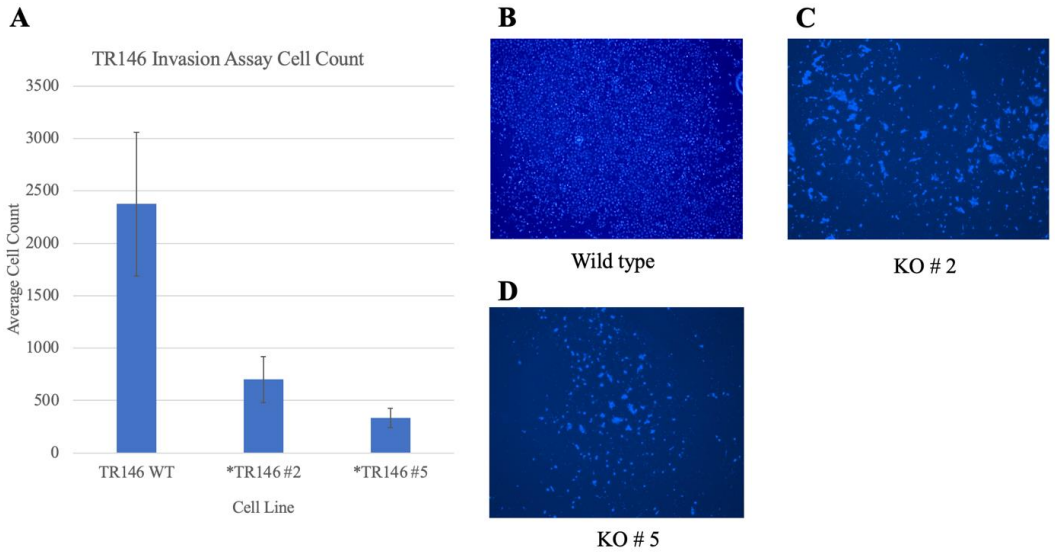

Figure 4. Invasion assay of TR146 WT and KO clones. Invasion through Matrigel matrix on inserts visualized with Calcein AM blue and quantified via ImageJ. A) Average invaded cell count for each cell line. B) WT TR146. C) TR146-KO #2 ($p = 0.02$). D) TR146-KO #5 ($p = 0.003$). * Indicates statistical significance ($p \leq 0.05$) as compared to TR146 WT; standard error bars were calculated across multiple day and intra-day replicates.

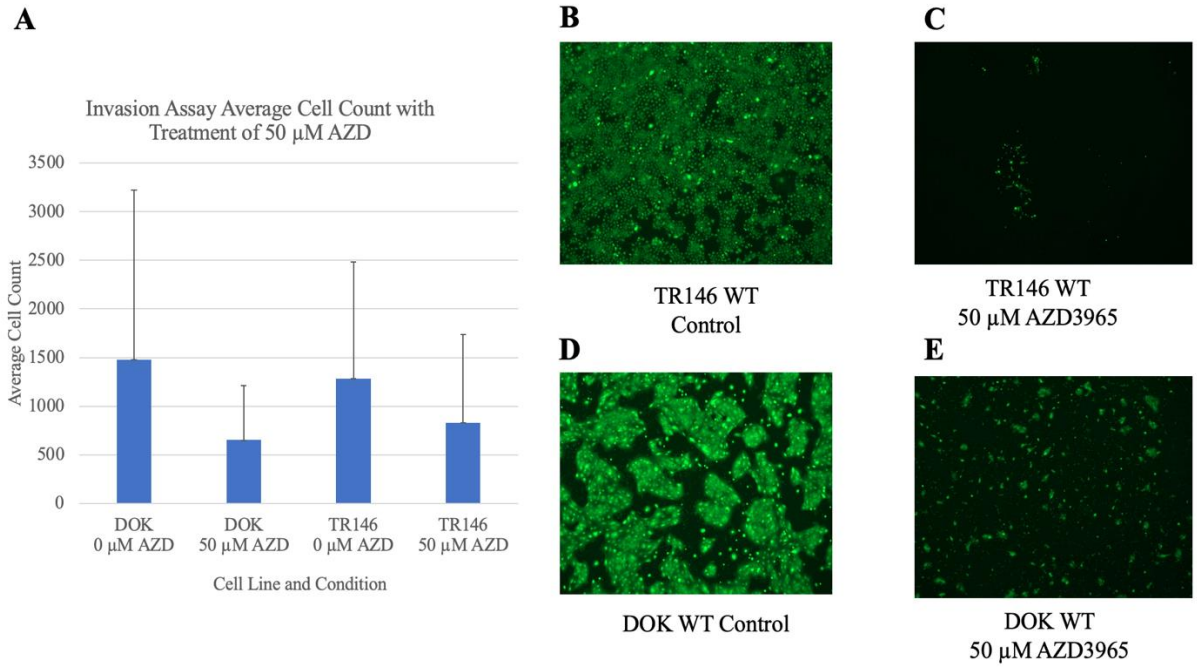

Figure 5. Invasion assay of TR146 and DOK WT cell lines with treatment of AZD3965. Invasion through Matrigel matrix on inserts visualized with Calcein AM green and quantified via ImageJ. A) Average invaded cell count for each cell line and condition. B) WT TR146 control. C) WT TR146 treated with 50 µM AZD3965. D) WT DOK. E) WT DOK treated with 50 µM AZD3965. Standard error bars were calculated across multiple day and intra-day replicates.

different harvests of cells provided inconsistent results and limited differences in invaded cells (not shown). Quantitation of cell invasion showed a general decrease in cell count when cells were treated with AZD3965, but not consistently throughout all replicates. Statistical analysis was unable to provide a significant difference when comparing treated versus untreated groups.

Discussion

This study provides evidence that reduced expression of MCT1 or pharmacological inhibition of its activity diminishes the invasive capacity of HNSCC cells, supporting the premise that MCT1 plays a role in the progression of head and neck cancer. To evaluate the role of MCT1 in HNSCC progression, genetic KO of MCT1 was performed in TR146 invasive HNSCC and DOK dysplastic cell lines for its gene, *SLC16A1*. *SLC16A1* KO using CRISPR/Cas9 editing resulted in significant decreases in expression at the mRNA and protein levels. Expression at the transcription level was determined using qRT-PCR, which showed large decreases in *SLC16A1* between WT controls and KO samples for both theTR146 and DOK cell lines. TR146 KO clones #2 and #5 showed almost complete loss of expression by qRT-PCR. DOK cell lines showed similar results with large decreases in *SLC16A1* expression compared to WT controls. Loss of protein expression was confirmed by immunoblotting. No detectable expression of MCT1 was observed in the KO clones generated for either the TR146 or DOK cell lines. Overall, qRT-PCR and immunoblotting results showed that MCT1 expression was significantly decreased in both TR146 and DOK cell lines using our gene editing approach.

Expression levels of *LAMC2* and *INHBA* were then measured to a draw correlation between *SLC16A1* KO and previously identified HNSCC invasion marker genes. *LAMC2* is involved in cell-cell interaction and migration and has previously been found to be an effective marker for HNSCC, allowing for distinction between cancerous and normal tissue (Chen et al., 2008). In addition, *INHBA* encodes a subunit of a ligand within the TGF-β family and has also been shown to be upregulated in and serve as a marker for HNSCC (Wu et al., 2019). Therefore, both *LAMC2* and *INHBA* were expected to decrease in response to *SLC16A1* KO, signifying a decrease in the tumorgenicity, or cancer-like properties, of the KO clones. For TR146 cells, we found that *LAMC2* was decreased in our KO cell lines, supporting the idea that an invasive phenotype is associated expression of *SLC16A1* and providing evidence to support the downstream molecular signaling effects of *SLC16A1* KO. Unexpectedly, the expression of *INHBA* was generally increased in TR146 KO cell lines which could be attributed to cell line-specific variation in expression of *INHBA*. In addition, many routes of dysfunction of the TGF-β signaling pathway have been found to exist in HNSCC, which could affect how cells express *INHBA* (Pring et al., 2006).

DOK KO lines showed decreases in *SLC16A1* expression similar to that observed in our TR146 KO clones, but in contrast to TR146 KO cells, the relationships between *LAMC2* and *INHBA* were not consistent. *LAMC2* expression was increased in the DOK

KO cell lines, as compared to WT controls, and *INHBA* did not show a distinct relationship between the WT and KO cells. Compared to cancerous TR146 WT cells, the expression of *SLC16A1* and *LAMC2* were significantly lower in DOK WT cells, reflecting the pre-cancerous state (dysplasia) of the DOK line. This data supports expectations of elevated malignancy of TR146 cells compared to DOK cells as each of these genes are upregulated in HNSCC and serve as markers for advanced disease. A lack of decreased *LAMC2* in DOK cell lines could be explained by the pre-cancerous state as expression is already lower in these samples, resulting in a reduced effect of *SLC16A1* KO in causing changes in the *LAMC2* expression profile. The expression of *INHBA* was higher in DOK samples, which could be related to the reversal of TGF-β tumor suppressor function to oncogenic function, as TGF-β signaling pathways have been characterized with both functions (Pardali and Moustakas, 2007). These preliminary results suggest that *SLC16A1* expression can affect other markers of tumorgenicity, but further investigation needs to be conducted to draw more concrete conclusions on the effect of *SLC16A1* KO on related HNSCC marker genes *LAMC2* and *INHBA*.

Upon validation of MCT1 KO, *in vitro* invasion assays were preformed to model cancer cell invasion into surrounding tissues. Results showed that loss of MCT1 expression decreases cancer cell invasion. Invasion in TR146 was dramatically reduced in TR146 KO clones #2 and #5, where MCT1 expression was significantly decreased. These results highlight the essential role MCT1 plays in invasion of HNSCC, and that genetic KO of this protein is sufficient to block invasion. We also assessed the impact of MCT1 expression on the invasive capacity of DOK cells. KO of MCT1 was carried out in these cell lines to evaluate early events in invasion before cancer occurs (dysplasia) and to evaluate MCT1 as a viable target for preventative therapies before dysplastic tissues progress toward early HNSCC. Our results here were inconclusive as consistent DOK invasion was not observed in our early invasion assays, preventing us from establishing a role for MCT1 in disease progression from dysplasia to early HNSCC.

Inhibition of MCT1 was achieved using a pharmacological inhibitor, AZD3965. AZD3965 has been tested in several other studies as a selective inhibitor of MCT1 in cancerous tissues (Beloueche-Babari et al., 2017; Polanski et al., 2014). While our results showed that treatment of the TR146 and DOK cell lines with AZD3965 blocked invasion in multiple experiments, decreased invasion was not consistently observed in all invasion assays and our findings did not reach statistical significance. This could imply activation of short-term compensatory mechanisms that act against inhibition of monocarboxylate transport, and these may depend on biological variations in the cell environment that naturally exist over time. Serum starvation of cells prior to invasion could deliver more consistent results for our invasion assays when testing for the effect of MCT1 inhibition through treatment of AZD3965 as well as genetic KO.

In summary, both genetic KO and pharmacological inhibition of MCT1 showed that disrupting the function of MCT1 limits

invasion of HNSCC and suggests that both genetic and pharmacological therapies may be effective in treating this disease. Additional studies addressing the role of MCT1 in promoting the invasion and progression of oral dysplasia toward early HNSCC will need to be completed along with a more complete assessment of the downstream signaling events regulated by MCT1 activity. Further examination of AZD3965 on the effects of MCT1 inhibition via 3-dimensional organoid or organotypic culture assays may provide more significant evidence for decreased invasion since these approaches more closely model tissues compared to standard 2-dimensional cell culture assays. MCT1 targeted therapies may also address the adaptability of CSCs and can provide specificity in HNSCC treatment because MCT1 is upregulated in CSCs (Khammanivong et al., 2014). By targeting CSCs, treatment resistance and cell adaptation may be greatly reduced and provide novel solutions for treating persistent cancers.

Acknowledgements

I would like to thank Drs. Ali Khammanivong and Erin Dickerson for their expert guidance and the Undergraduate Research Opportunities Program. Partial support for this project was provided by the Animal Cancer Care and Research program at the College of Veterinary Medicine.

References

Alsahafi, E., Begg, K., Amelio, I., Raulf, N., Lucarelli, P., Sauter, T., and Tavassoli, M. (2019). Clinical update on head and neck cancer: molecular biology and ongoing challenges. Cell Death & Disease 2019 10:8 *10*, 1–17.

Baniebrahimi, G., Mir, F., and Khanmohammadi, R. (2020). Cancer stem cells and oral cancer: insights into molecular mechanisms and therapeutic approaches. Cancer Cell International 2020 20:1 *20*, 1–15.

Beloueche-Babari, M., Wantuch, S., Galobart, T.C., Koniordou, M., Parkes, H.G., Arunan, V., Chung, Y.L., Eykyn, T.R., Smith, P.D., and Leach, M.O. (2017). MCT1 inhibitor AZD3965 increases mitochondrial metabolism, facilitating combination therapy and non-invasive magnetic resonance spectroscopy. Cancer Research *77*, 5913.

Brizel, D.M., Sibley, G.S., Prosnitz, L.R., Scher, R.L., and Dewhirst, M.W. (1997). Tumor hypoxia adversely affects the prognosis of carcinoma of the head and neck. International Journal of Radiation Oncology*Biology*Physics *38*, 285–289.

Chen, D., and Wang, C.-Y. (2019). Targeting cancer stem cells in squamous cell carcinoma. Precision Clinical Medicine *2*, 152–165.

Chen, C., Méndez, E., Houck, J., Fan, W., Lohavanichbutr, P., Doody, D., Yueh, B., Futran, N.D., Upton, M., Farwel, D.G., et al. (2008). Gene expression profiling identifies genes predictive of oral squamous cell carcinoma. Cancer Epidemiology, Biomarkers & Prevention : A Publication of the American Association for Cancer Research, Cosponsored by the American Society of Preventive Oncology *17*, 2152.

Cho, J.K., Hyun, S.H., Choi, N., Kim, M.J., Padera, T.P., Choi, J.Y., and Jeong, H.S. (2015). Significance of Lymph Node Metastasis in Cancer Dissemination of Head and Neck Cancer. Translational Oncology *8*, 119.

Curry, J.M., Tuluc, M., Whitaker-Menezes, D., Ames, J.A., Anantharaman, A., Butera, A., Leiby, B., Cognetti, D.M., Sotgia, F., Lisanti, M.P., et al. (2013). Cancer metabolism, stemness and tumor recurrence: MCT1 and MCT4 are functional biomarkers of metabolic symbiosis in head and neck cancer. Cell Cycle (Georgetown, Tex.) *12*, 1371–1384.

Halestrap, A.P. (2013a). Monocarboxylic Acid Transport. Comprehensive Physiology *3*, 1611–1643.

Halestrap, A.P. (2013b). The SLC16 gene family – Structure, role and regulation in health and disease. Molecular Aspects of Medicine *34*, 337–349.

Halestrap, A.P., and Meredith, D. (2004). The SLC16 gene family-from monocarboxylate transporters (MCTs) to aromatic amino acid transporters and beyond. Pflugers Arch-Eur J Physiol *447*, 619–628.

Johnson, D.E., Burtness, B., Leemans, C.R., Lui, V.W.Y., Bauman, J.E., and Grandis, J.R. (2020). Head and neck squamous cell carcinoma. Nature Reviews Disease Primers 2020 6:1 *6*, 1–22.

Khammanivong, A., Gopalakrishnan, R., and Dickerson, E.B. (2014). SMURF1 silencing diminishes a CD44-high cancer stem cell-like population in head and neck squamous cell carcinoma. Molecular Cancer *13*.

Khammanivong, A., Sorenson, B.S., Ross, K.F., Dickerson, E.B., Hasina, R., Lingen, M.W., and Herzberg, M.C. (2016). Involvement of calprotectin (S100A8/A9) in molecular pathways associated with HNSCC.

Krishnamurthy, S., and Nör, J.E. (2012). Head and neck cancer stem cells. J Dent Res *91*, 334–340.

Pardali, K., and Moustakas, A. (2007). Actions of TGF-β as tumor suppressor and pro-metastatic factor in human cancer. Biochimica et Biophysica Acta (BBA) - Reviews on Cancer *1775*, 21–62.

Picon, H., and Guddati, A.K. (2020). Mechanisms of resistance in head and neck cancer.

Polanski, R., Hodgkinson, C.L., Fusi, A., Nonaka, D., Priest, L., Kelly, P., Trapani, F., Bishop, P.W., White, A., Critchlow, S.E., et al. (2014). Activity of the Monocarboxylate Transporter 1 inhibitor AZD3965 in Small Cell Lung Cancer. Clinical Cancer Research : An Official Journal of the American Association for Cancer Research *20*, 926.

Prince, M.E., Sivanandan, R., Kaczorowski, A., Wolf, G.T., Kaplan, M.J., Dalerba, P., Weissman, I.L., Clarke, M.F., and Ailles, L.E. (2007). Identification of a subpopulation of cells with cancer stem cell properties in head and neck squamous cell carcinoma. Proceedings of the National Academy of Sciences of the United States of America *104*, 973–978.

Pring, M., Prime, S., Parkinson, E.K., and Paterson, I. (2006). Dysregulated TGF-β1-induced Smad signalling occurs as a result of defects in multiple components of the TGF-β signalling pathway in human head and neck carcinoma cell lines. International Journal of Oncology *28*, 1279–1285.

Rupniak, H.T., Rowlatt, C., Lane, E.B., Steele, J.G., Trejdosiewicz, L.K., Hill, B.T., Laskiewicz, B., and Povey, S. (1985). Characteristics of Four New Human Cell Lines Derived From Squamous Cell Carcinomas of the Head and Neck. JNCI: Journal of the National Cancer Institute *75*, 621–635.

Sayed, S.I., Dwivedi, R.C., Katna, R., Garg, A., Pathak, K.A., Nutting, C.M., Rhys-Evans, P., Harrington, K.J., and Kazi, R. (2011). Implications of understanding cancer stem cell (CSC) biology in head and neck squamous cell cancer. Oral Oncology *47*, 237–243.

Siegel, R.L., Miller, K.D., and Jemal, A. (2017). Cancer Statistics, 2017. CA: A Cancer Journal for Clinicians *67*, 7–30.

Sonveaux, P., Végran, F., Schroeder, T., Wergin, M.C., Verrax, J., Rabbani, Z.N., de Saedeleer, C.J., Kennedy, K.M., Diepart, C., Jordan, B.F., et al. (2008). Targeting lactate-fueled respiration selectively kills hypoxic tumor cells in mice. The Journal of Clinical Investigation *118*, 3930–3942.

Stein, A.P., Saha, S., Kraninger, J.L., Swick, A.D., Yu, M., Lambertg, P.F., and Kimple, R. Prevalence of human papillomavirus in oropharyngeal cancer: a systematic review.

Wu, Z. hong, Tang, Y., Niu, X., and Cheng, Q. (2019). Expression and gene regulation network of INHBA in Head and neck squamous cell carcinoma based on data mining. Scientific Reports 2019 9:1 *9*, 1–11.